

Assessment of signal processing methods for measuring the respiratory rate in the neonatal intensive care unit

João Jorge, *Member, IEEE*, Mauricio Villarroel, Sitthichok Chaichulee, *Member, IEEE*, Gabrielle Green, Kenny McCormick, and Lionel Tarassenko

Abstract—Knowledge of the pathological instabilities in the breathing pattern can provide valuable insights into the cardiorespiratory status of the critically-ill infant as well as their maturation level. This paper is concerned with the measurement of respiratory rate (RR) in premature infants. We compare the rates estimated from (a) the chest impedance pneumogram, (b) the ECG-derived respiratory rhythms, and (c) the PPG-derived respiratory rhythms against those measured in the reference standard of breath detection provided by attending clinical staff during 165 manual breath counts. We demonstrate that accurate RR estimates can be produced from all sources for RR in the 40 - 80 bpm (breaths per min) range. We also conclude that the use of indirect methods based on the ECG or the PPG poses a fundamental challenge in this population due to their poor behaviour at fast breathing rates (upwards of 80 bpm).

Index Terms—electrical impedance pneumography, electrocardiogram, NICU, Paediatrics, physiological monitoring, photoplethysmogram, respiratory rate.

I. INTRODUCTION

THE neonatal intensive care unit (NICU) is an intensive care and high-dependency unit offering specialist care for critically-ill or premature newborn infants. Respiratory conditions are the most common reason for admission to a NICU in both term and preterm infants [1]. Overall, it is estimated that between 2.2% [2] to 6.7% [3] of all births are complicated by a respiratory disorder. In fact, one study reported that, with the exception of infants with syndromes and those with congenital or surgical conditions, 33.3% of all neonatal admissions at > 28 weeks of gestation had respiratory disorders as their primary reason for admission [4]. A further study estimated that 20.5% of all neonatal admissions showed signs of respiratory distress [5]. Evidence of increasing rates of neonatal admissions due to respiratory disorders has also been reported [6].

The clinical signs of respiratory disorders are thus important to recognise. Most respiratory conditions have some manifestation in the respiratory signal, namely in the morphology or frequency of this

signal (*i.e.* the respiratory rate). Continuous monitoring of respiratory rate (RR) in neonatal units is generally done by electrical impedance pneumography (IP). IP is a convenient method in this setting as patients are already monitored by electrocardiography, but is prone to inaccurate readings due to a number of factors including poor probe placement, motion artefact, and physiologic events which cause thoracic movements unrelated to breathing (such as coughing, or crying) [7, 8]. The high prevalence of noise and high false alarm rates means that respiratory signals are still largely disregarded in neonatal intensive care units. There is, therefore, a pressing need to improve the reliability of RR monitoring in these units.

In adherence to clinical care standards, preterm infants admitted to a NICU undergo continuous monitoring of heart rate (HR) acquired using the electrocardiograph, and peripheral blood oxygen saturation (SpO₂) acquired using pulse oximeters. The cardiosynchronous signals collected by such devices – the electrocardiogram (ECG) and the photoplethysmogram (PPG) – have been shown to exhibit amplitude and frequency oscillations that reflect the respiratory cycle [9–11]. The ubiquitousness of ECG and PPG monitors in neonatal units could provide an opportunity for concurrent RR monitoring if sufficiently robust signal processing methods to estimate RR from these two signals were available.

Algorithms for the estimation of RR from the ECG and the PPG were first reported in 1985 [10] and 1992 [12], respectively. Although a considerable amount of work on this topic has since been reported, to our knowledge no study has been published which assesses the reliability of RR estimates provided by indirect methods based on the ECG or PPG records of spontaneously breathing neonates. As a result, the applicability of their results to the monitoring of these patients faces several limitations. The first limitation is the range of RR values reported; as datasets consist solely of records from adults [10, 12–25] or older children [26, 27], the range of RR values in the training and test sets is concentrated in the interval from 5 to 25 bpm (breaths per min), a range much lower and narrower than that observed in preterm and newborn infants (Fig. 1b). For this reason, results from these studies are not necessarily representative of the behaviour of the methods in our patient group. In addition, no paper evaluates the performance of their methods against the reference standard of manual respiratory assessments by clinical experts.

This paper is concerned with the measurement of RR in preterm infants. We compare RR values estimated from (a) the electrical impedance pneumogram recorded with the ECG electrodes, (b) the ECG-derived respiratory rates, and the (c) PPG-derived respiratory rates against those measured using the reference standard of breath detection provided by attending clinical staff during manual breath counts. In the case of both ECG- and PPG-derived respiration, we consider both amplitude and frequency modulations of the waveforms by the respiratory cycle and fuse the estimates from all sources of modulation to obtain a single RR estimate from each device for each time window.

The rest of this paper is organised as follows: Section II introduces the dataset and III the proposed methodology. The results of RR estimation are reported in Section IV and discussed in Section V. The main conclusions are presented in Section VI.

Manuscript received Month X, 201X; revised Month X, 201X; accepted Month X, 201X. Date of publication Month X, 201X; date of current version Month X, 201X. The work of J. Jorge and S. Chaichulee was supported by the the RCUK Digital Economy Programme, grant number EP/G036861/1 (Oxford Centre for Doctoral Training in Healthcare Innovation). J. Jorge also acknowledges Fundação para a Ciência e Tecnologia, Portugal, doctoral grant SFRH/BD/85158/2012. S. Chaichulee acknowledges the National Science and Technology Development Agency, Thailand. M. Villarroel was supported by the Oxford Centre of Excellence in Medical Engineering funded by the Wellcome Trust and EPSRC under grant number WT88877/Z/09/Z. K. McCormick was supported by the NIHR Biomedical Research Centre Programme, Oxford.

J. Jorge is with the Institute of Biomedical Engineering, Department of Engineering Science, University of Oxford, Oxford OX3 7DQ, U.K. (e-mail: joao.jorge@eng.ox.ac.uk).

M. Villarroel and S. Chaichulee are with the Institute of Biomedical Engineering, Department of Engineering Science, University of Oxford, Oxford, UK.

K. McCormick is with the Neonatal Unit, John Radcliffe Hospital, Oxford University Hospitals Trust, Oxford, UK.

L. Tarassenko is with the Institute of Biomedical Engineering, Department of Engineering Science, University of Oxford, Oxford, UK.

TABLE I: Selected population demographics of the subgroup of infants enrolled in the NICU study. Gestational age and weight are reported for the first day of recording.

| Subject | Gender (M/F) | Ethnicity [†] | Gestational age (weeks + days) | Weight (g) | Record (days) |
|---------|--------------|------------------------|--------------------------------|------------|---------------|
| 1 | M | WB | 34+2 | 1210 | 4 |
| 2 | M | WA | 31+2 | 1510 | 2 |
| 3 | M | WB | 31+0 | 1380 | 3 |
| 4 | F | WB | 30+4 | 1270 | 2 |
| 5 | M | WB | 32+1 | 1680 | 3 |

[†]WB = White-British; WA = White and Asian.

II. DATA COLLECTION

Data for this study was acquired during an observational study in the NICU at the John Radcliffe Hospital (MONITOR Study - Research Ethics Committee: 13/SC/0597). This study involved the recruitment of 30 preterm infants of less than 37 weeks of corrected postmenstrual age. Each preterm infant was recorded for up to four consecutive days. During this period, we recorded the physiological signals and vital sign data collected by the patient monitor as part of routine care (Fig. 1). The main focus of this paper is on the periods of manual measurements of respiration available for the last five study subjects in this dataset (PN 26-30). The main demographic characteristics of this subgroup are reported in Table I.

A. Signal acquisition

All conventionally-monitored signals were recorded using an IntelliVue[®] MX800 Revision J, 2013 patient monitor (Philips, Amsterdam, Netherlands) and relayed to a separate workstation, a standard PC with a 4TB disk and 8GB RAM under Windows 7 (using ixTrend[®], ixElevance GmbH, Wildau, Germany) via R-232 serial transmission.

Using the MX800 patient monitor built-in software, the infant's vital signs are derived from the raw physiological signals collected and reported at a rate of 1 estimate per second. Baseline values for the monitored vital signs are shown in Fig. 1. RR was estimated from the bipolar IP signals collected at 62.5Hz using the set of neonatal chest electrodes provided with the monitor. HR was estimated from the single-lead ECG signal (sampled at 250Hz) acquired using the same pair of electrodes and a reference electrode placed on the infant's abdomen, and SpO₂ was estimated from the PPG signal acquired by

a SET LNCS Neo[®] foot oximetry probe (Masimo Corporation, Irvine, USA) and sampled at 125 Hz.

B. Manual measurements

For the breath counts performed on the last five infants recruited, the clinical staff were instructed to press a set key (Spacebar) on the keyboard of the study workstation at the time each breath was registered. Each key press was logged electronically using a custom keylogger. Each manual count cycle consists of a train of 40 time-stamped breaths. In the event of excessive movement by the infant or fading breathing motion rendering individual chest excursions visually indistinguishable over the course of an ongoing counting cycle, the current count was aborted and a new one was restarted once the infant settled and visible breathing movements resumed. A total of 165 valid manual counts were available (see Appendix I).

III. DATA ANALYSIS

This section presents the signal processing methods used for estimating RR and signal quality indices (SQIs) for the acquired physiological signals. Our general approach to deriving these quantities is shown schematically in Fig. 2. For each block (covered in more detail in Sections III-A through III-C) we have selected methods whose performance has been tested on annotated datasets available in the public domain. These datasets, which normally consist of physiological signals collected from adult patients in intensive care, are often used in biomedical research to guide the selection of appropriate method parameters. This can affect the overall performance of the developed automated methods in other patient groups with different ages or cardiovascular health. Thus, some method parameters were adjusted to address the unique physiology of the neonatal population based on domain knowledge of clinical experts. Instances where any parameters used in the authors' original implementation were modified have been indicated in the main text.

The fast-changing respiratory rates observed in the preterm infant mean that this vital sign can change considerably over the course of the time interval conventionally allocated to manual breath counts (*i.e.* 60 seconds). We felt that a comparison of the RR values computed at the end of each counting cycle would fail to capture the full dynamic range of this vital sign and convey the false impression that this signal remains approximately constant over such a period. Thus, in this analysis, we opted instead to segment the periods of manual breath counts into shorter time windows of 8 seconds and perform a comparison of the RR computed over these 8-second windows.

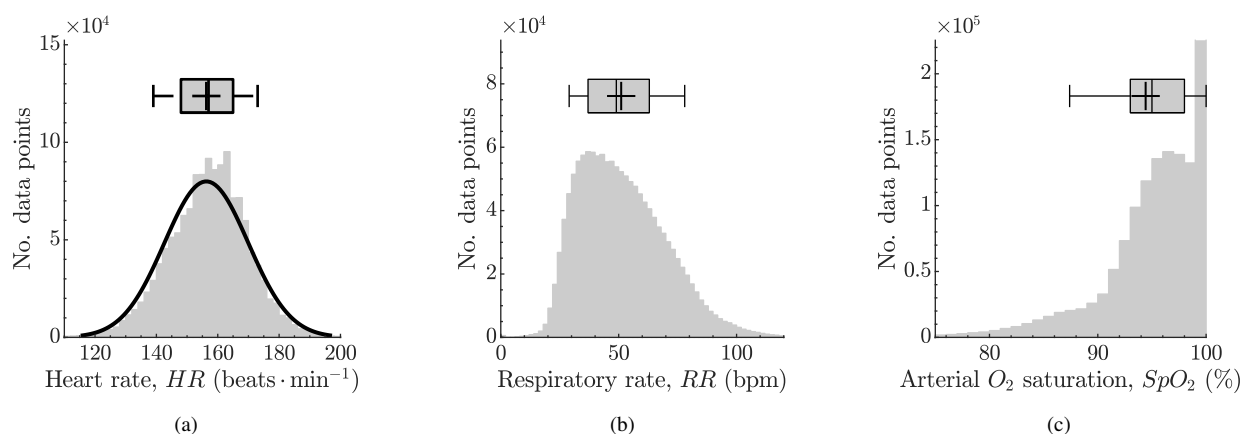


Fig. 1: Histograms of reference vital signs of the infants recruited: (a) Heart rate derived by the patient monitor from ECG, (b) respiratory rate derived by the patient monitor from IP, and (c) SpO₂ derived by the pulse oximeter. + is the data mean, the boxplot bounds the 25 % and 75 % quartiles and the whiskers bound the 9 % and 91 % of the data. The black curve in (1a) shows a normal fit to the data.

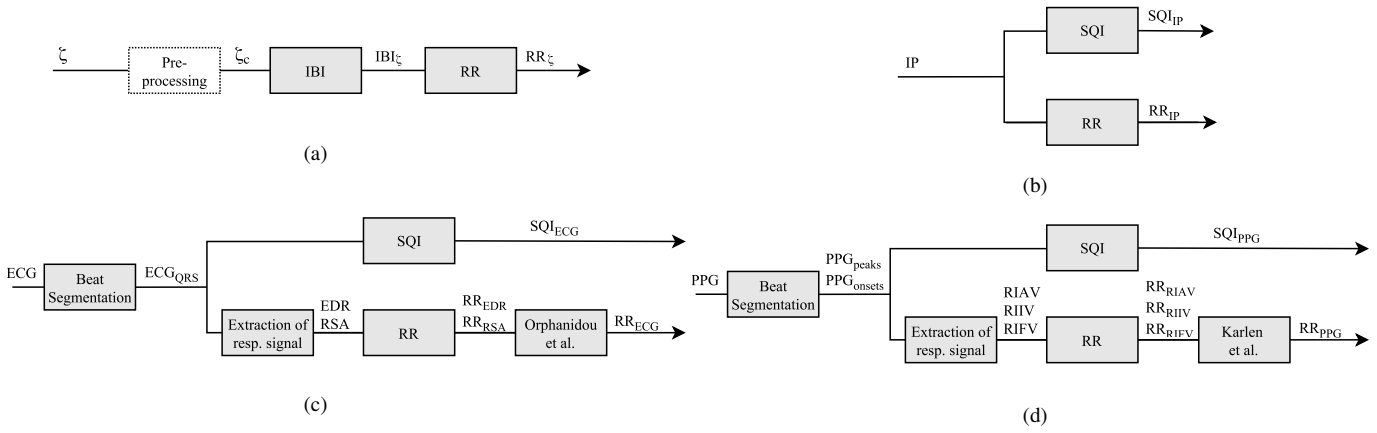


Fig. 2: Computation of the respiratory rate and signal quality indices. (a) As a reference for RR, we computed this quantity from the instantaneous breath information obtained during manual respiratory measurements. (b) - (d) Respiratory rates were computed from all the collected signals. (b) A signal quality index for IP signal (SQI_{IP}) was also considered. Cardiac beats were segmented from (c) ECG and (d) PPG waveforms; then, signal quality measures (SQI_{ECG} , SQI_{PPG}) and surrogate respiration signals were derived. Other quantities in the diagram are introduced later in this paper.

A. Segmentation of cardiac beats

The segmentation of cardiac beats in the ECG or PPG signals relies upon the occurrence of characteristic waveform patterns in these time series that are synchronous with the cardiac cycle (QRS complexes in the ECG and the blood-volume pulse in the PPG). Thus, by segmenting the raw signals at fiducial points within these repeating units, one can obtain single-beat waveforms from:

ECG ECG beat detection was performed using the well-known Hamilton and Tompkins algorithm [28]. The *wqrs* beat detector by [29] was also implemented, given its role (alongside the Tompkins detector) in the definition of ECG signal quality index described in Section III-B. Both algorithms have shown high accuracy in previous studies using the single-channel ECG records in the MIT-BIH Arrhythmia database [30] (99.3% for Tompkins et al., and 99.7% for Zong et al.).

In our computation of the location of the R-peaks using the *wqrs* open-source QRS detector, we shortened the refractory period used by [29] to half this value (125 ms) to accommodate for the higher heart rates observed in neonates (as evidenced in Fig. 1a).

PPG Much previous work exists concerning the segmentation of the PPG into arterial cardiac pulses from reference points in this waveform [31–34]. We implemented three methods available in the public literature for beat pulse segmentation (*WABP* [31], Li *et al.* [33], and Karlen *et al.* [34]) and analysed their results on the PPG records of a subset of 12 subjects. As an outcome of this analysis, we observed that the three methods produced similar results on this subset, as evidenced by the high $b \times b$ scores between matched peak locations for all possible pairings of the three methods: $(b \times b)_{WABP \times Li} = 0.95$, $(b \times b)_{WABP \times Karlen} = 0.98$, $(b \times b)_{Li \times Karlen} = 0.96$. The statistics reported are mean $b \times b$ scores computed over 30-second time windows with no overlap.

In the following sections, we used the PPG peak and onset locations provided by Karlen *et al.*'s method for PPG pulse segmentation, which showed marginally faster running times on the machine used for data analysis.

B. Computation of signal quality indices

The use of reliable signal quality indices (SQIs) is of fundamental importance as a pre-processing step to signal analysis so that the latter is only attempted in epochs for which the recorded signals communicate adequate representations of the underlying physiological mechanisms. The following SQIs were implemented:

SQI_{IP} The metric adopted for determining the quality of IP signals, spectral purity (Γ_s), was derived from the EEG domain. Its use as a measure of signal periodicity was first proposed by [35] in EEG studies and later extended to other physiological signals [36] and successfully applied to IP signals [25, 37].

Γ_s is a heuristic related to the Hjorth descriptors [38] (namely the complexity descriptor \mathcal{H}_3), which describe the spectrum of a signal in terms of its moments. The n^{th} order spectral moment $\bar{\Omega}_n$ of a signal is given by the integral

$$\bar{\Omega}_n = \int_{-\pi}^{\pi} \Omega^n \mathcal{P}_w(e^{j\Omega}) d\Omega \quad (1)$$

where $\mathcal{P}_w(e^{j\Omega})$ is the power spectrum of the windowed signal and Ω is the angular frequency ($\Omega = 2\pi f$, with f in physical frequency units). Γ_s is defined as the ratio between the squared 2nd order moment, and the product of the 0th order moment (*i.e.* the total power) and 4th order moment [39]:

$$\Gamma_s = \frac{\bar{\Omega}_2^2}{\bar{\Omega}_0 \bar{\Omega}_4} \quad (2)$$

Γ_s is designed to reflect the bandwidth of the signal, *i.e.* how well the signal may be described by a periodic signal with a single dominant frequency. Following (2), Γ_s is a strictly positive quantity with a maximum value of unity for a sinusoidal signal. To obtain SQI_{IP} we computed Γ_s over sliding windows of 30 seconds with a 1-second shift between windows. Γ_s was estimated using the temporal expressions of the spectral moments.

SQI_{ECG} In clinical ECG analysis, a great deal of emphasis has been placed on the definition of SQI metrics to reduce

false alarm rates in adult intensive care units (ICUs). With this in mind, most definitions of ECG signal quality found in the literature have been developed for adult ICU patient data, particularly in the work of [40–42]. In our analysis, in order to assess the quality of ECG records, the SQI defined in [41] was applied as originally implemented by the authors with the exception of the following: (a) when assessing the quality of the single-lead ECG signal $bSQI$ (Section 2.1.1, Eq.1 in [41]), a shorter tolerance interval $\xi = 50$ ms was adopted for computing the ratio of beats detected synchronously by both QRS detection algorithms, and (b) as a single ECG lead was available, the multiple lead $iSQI$ (Section 2.1.2, Eq.2 in [41]) was set to $iSQI = 1$. The former parameter change is justified by the higher heart rates observed in neonates.

SQI_{PPG} To assess the reliability of PPG signals we followed the morphological approach by Li *et al.* [43]. Li *et al.*'s SQI index, or SQI_{PPG}^* , takes as input parameters the peak or onset locations that segment each beat in order to build a dynamic beat template. In our implementation, the peak locations were found using the methods in Section III-A. In addition, the minimum and maximum beat-to-beat intervals used by [43] were shifted to 0.5 and 1.5 s, respectively. These values correspond to the inverse of the limits of the aforementioned neonatal respiratory range ([40; 120] bpm). SQI_{PPG}^* obtained in this way is defined on a beat basis. A window-based $SQI_{PPG}(w)$ was calculated as the mean SQI_{PPG}^* score over the cardiac beats in the analysis window w .

C. Extraction of respiratory signals

The physiological signals collected in the NICU fall into two categories. Some measure the respiration signal explicitly, either in the shape of tidal flow (*e.g.* capnography), changes in intrathoracic volume or resistivity (*e.g.* electrical impedance pneumography) or other measurand from which the respiratory waveform can be directly extracted, whereas in others, such as the physiological signals monitored more routinely (*e.g.* ECG or PPG), respiration exerts only a modulatory effect on the original signal. Thus, a fundamental step in the estimation of RR from the ECG and PPG is the extraction of the respiratory signal from the amplitude and frequency modulation of these waveforms. In the following analysis, ECG and PPG-derived respiratory signals were derived over 8-second windows with 1-second shifts. As a result of this procedure, 3799 time windows were available for respiratory rate estimation. To facilitate comparison between the estimated respiratory rates and the reference manual rates, these windows were defined so that they overlapped with those used in the computation of manual respiratory rates RR_{ζ} .

ECG ECG-derived respiration can be obtained from two effects: changes in beat morphology and respiratory sinus arrhythmia (RSA).

The methodology for extracting respiratory information from changes in beat morphology was first explored in the seminal paper by Moody *et al.* [10], which measured the oscillation in the ratio of the QRS areas measured in two ECG leads as a measure of respiratory activity. There has since been a surge of interest in this topic resulting in a multitude of signal processing algorithms to derive respiratory-induced modulations from multi-lead ECG signals [44,45]. In this study, a single ECG lead was available. Given the precedent of its use in neonatal ECG data [37] in contrast to recent methods, we adopt

the approach based on QRS area summation pioneered by Moody *et al.* [10] to obtain the ECG-derived respiration signal (EDR) from the ECG records.

The second approach relies on the well-known modulation of heart rate by the respiratory effort through respiratory-induced pressure changes in the main and peripheral arteries. These variations in the instantaneous heart rate are governed by the respiratory sinus arrhythmia and may be extracted as the time series of beat-to-beat R - R intervals (henceforth RSA^*) [20–23,46]. The R - R intervals in the analysis window w were calculated as the difference between the times of successive R -peaks (found using [28]).

Finally, both the EDR^* and RSA^* time series were linearly interpolated at a sampling rate of 4 Hz to obtain the evenly-sampled time series EDR and RSA , respectively.

PPG

Respiratory-led fluctuations in the PPG signal can be decomposed into three fundamental modulations of this waveform [11]. Often the preferred methods to extract respiration from this signal consist in a combination of these modulations [13] and that is the approach we adopt here. Given a PPG record segmented into a series of peaks and troughs by the algorithm in Section III-A, the following rhythms were computed as surrogates of the respiratory signal [25]:

- $RIIV^*$ (Respiratory-induced intensity variations) consisting of the time series of PPG peak amplitudes;
- $RIAV^*$ (Respiratory-induced amplitude variations) consisting of the time series of amplitude differences between the peak and the onset of a PPG pulse;
- $RIFV^*$ (Respiratory-induced frequency variations) consisting of the time series of intervals between consecutive PPG peaks. This quantity was inverted to reflect frequency variations.

The $RIIV^*$, $RIAV^*$ and $RIFV^*$ time series were then linearly interpolated at a sampling rate of 4 Hz to obtain the evenly-sampled time series $RIIV$, $RIAV$ and $RIFV$.

D. Estimation of respiratory rate

1) *from manual breath counts*: As a reference for RR, we computed this quantity from the instantaneous breath measurements obtained during manual respiratory assessments (Fig. 2a). The timestamps of key presses during the study sessions were parsed into separate counting cycles in the manner described in Appendix I. In summary, a total of 209 independent counting cycles were recorded. Out of these, 39 breath counts were aborted by the clinical staff due large infant movements, wriggling motion, or other causes. Out of the remaining measurements, 5 were recorded when the monitoring equipment was not in operation. This left a total of 165 manual breath counts, or 6924 events if individual breaths are considered.

We modelled each counting cycle c as series of n_c breaths defined by a train of spikes $\zeta_c(t)$ at instants, $t_0^c, \dots, t_{n_c-1}^c$ which mark the timing of individual breaths. These time instants may correspond to either expiration or inspiration end times:

$$\zeta_c(t) = \begin{cases} 1, & \text{if } t \in t_0^c, \dots, t_{n_c-1}^c \\ 0, & \text{otherwise} \end{cases} \quad (3)$$

The choice between selecting the end-inspiratory or the end-expiratory pause as the onset of each respiratory cycle was left at the discretion of the nursing staff performing the manual count. Therefore,

this choice was consistent within the same manual counting cycle but not across cycles. The $n_c - 1$ inter-breath intervals, $IBI_\zeta(t)$, were then computed trivially as the time differences between consecutive breaths and assigned the timestamp of the later breath:

$$IBI_\zeta(t_n^c) = t_n^c - t_{n-1}^c, n \in \{1, \dots, n_c - 1\} \quad (4)$$

For each c , the start of the first analysis window was set to t_0^c . The last window for this cycle was the last one whose right limit was below $t_{n_c-1}^c$. For each time window w , $RR_\zeta(w)$ was computed as the inverse of $\bar{IBI}_\zeta(w)$, the mean value of the IBI_ζ data points within the window and assigned the timestamp corresponding to the centre time point of the window.

2) from derived respiratory rhythms: The respiratory rate was derived for each source through analysis of the spectral content of the respiratory signals extracted for each window. Many techniques are available to do this; we adopted an auto-regressive (AR) model due to its superior frequency resolution over traditional (non-parametric) methods based on the Fast Fourier Transform (FFT) periodogram [47]. Prior to model-fitting, it is useful to remove the baseline wander and high-frequency noise. This was achieved through the use of digital filters. The respiratory time series were filtered using a 40th order (*i.e.* a 10-second long) bandpass, linear phase, finite impulse response (FIR) filter, using a Hamming window and cut-off frequencies which encompass the range of plausible respiratory rate values for the population under study (20 - 140 bpm). A 9th order AR model was then fitted to the filtered waveforms using Burg's algorithm [48]. The frequency corresponding to the peak of the autoregressive power spectral density function in the aforementioned range of frequencies was taken as the respiratory rate estimate and represented by

$$RR_i, i \in \{IP, EDR, RSA, RIIV, RIAV, RIFV\} \quad (5)$$

where the subscript index i refers to the original respiratory signal from which this rate was computed.

The challenges placed on indirect methods of extracting the respiratory signal are aggravated in real-life monitoring scenarios. For this reason, a post-processing stage, whereby simultaneous RR estimates corresponding to different modulations of the same source are fused, received particular attention:

RR_{ECG} A fused ECG-derived estimate of respiratory rate $RR_{ECG}(w)$ for window w was selected among $\{RR_{EDR}(w), RR_{RSA}(w)\}$, using the pole magnitude criterion [14]. The RR estimate was chosen as the frequency of the highest magnitude pole of the two 9th order AR models obtained from auto-regressive spectral analysis of the resampled EDR and RSA respiratory signals.

RR_{PPG} A fused PPG-derived respiratory rate $RR_{PPG}(w)$ was estimated using the approach in Karlen *et al.* [13] as the mean of the three respiratory-induced variations derived from PPG $\{RR_{RIIV}(w), RR_{RIIV}(w), RR_{RIFV}(w)\}$. In compliance with the authors, for windows for which the standard deviation of the three estimates exceeds 4 bpm, no RR estimate was provided (*i.e.* $RR_{PPG}(w) = 0$).

E. Error analysis

For a quantitative comparison between the performance of the methods implemented, the mean absolute error (MAE), the error means (bias), and standard deviation (SD) of RR estimates were computed against RR_ζ .

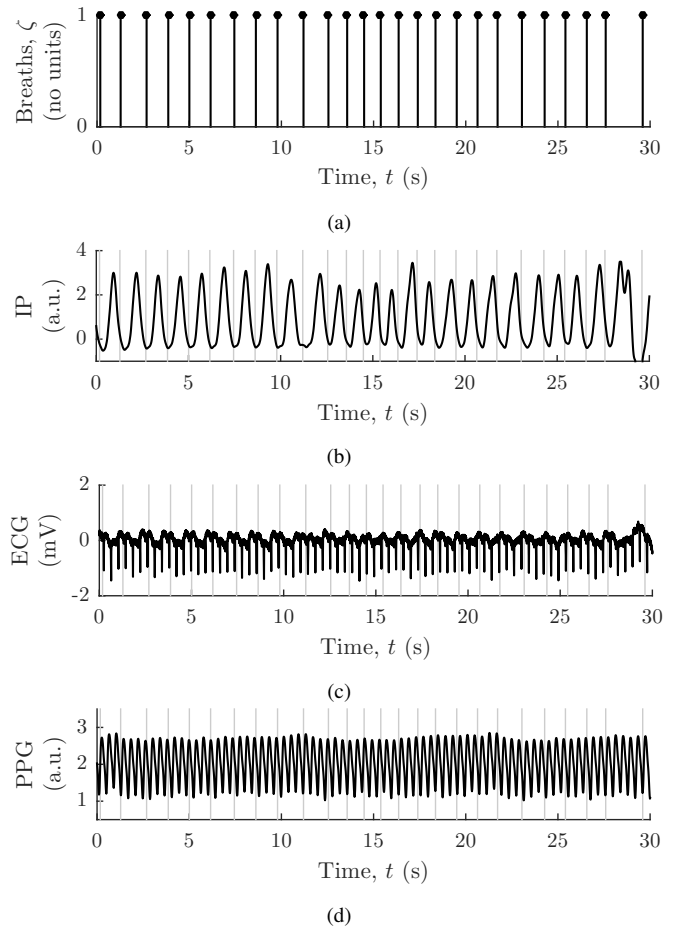


Fig. 3: An example of (b) IP, (c) ECG, and (d) PPG signals during a manual counting cycle on PN 28. Modulation through 25 complete respiratory cycles is shown. The (a) manually-counted breaths on the upper trace are reproduced as grey vertical lines on the subsequent plots.

IV. RESULTS

Fig. 3 shows the IP signal and the respiratory-induced modulation of ECG and PPG signals through a sample of 25 complete respiratory cycles. The modulation of the R-peak and the changes in IP with ventilatory effort are clearly seen. Less evident in this segment is the amplitude modulation of PPG with respiration.

A. Respiratory rate from direct methods

In Fig. 4, we compare the accuracy of re-derived RR_{IP} and the RR estimates provided by the patient monitor from the same source (RR_{MON}). By default, the monitor estimates are given at 1-second intervals. For comparison, these were interpolated at the time instants of the RR_{IP} data points.

We observe that the MAE of both RR_{IP} and RR_{MON} estimates decrease monotonically when only estimates from windows with progressively higher thresholds in SQI_{IP} are considered. In spite of the increase in accuracy achieved through SQI thresholding, a considerable difference in the error performance between the two methods persists with $MAE(RR_{IP}) = 6.7$ bpm and $MAE(RR_{MON}) = 11.2$ bpm at $SQI_{IP} \geq 0.75$. At this SQI threshold, respiratory rates were computed for 67.3% of the IP windows.

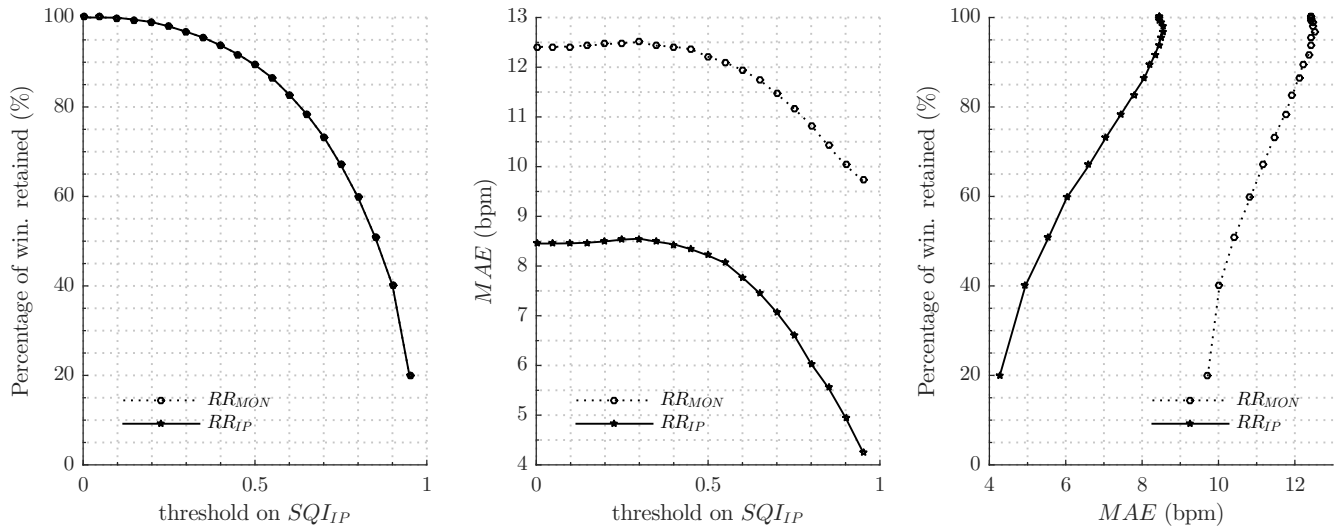


Fig. 4: Relationship between the threshold on SQI_{IP} , the percentage of windows retained and the mean absolute error (MAE) of retained RR_{IP} and RR_{MON} estimates against RR_{ζ} during manual breath counts. RR_{MON} are the RR estimates provided by the patient monitor.

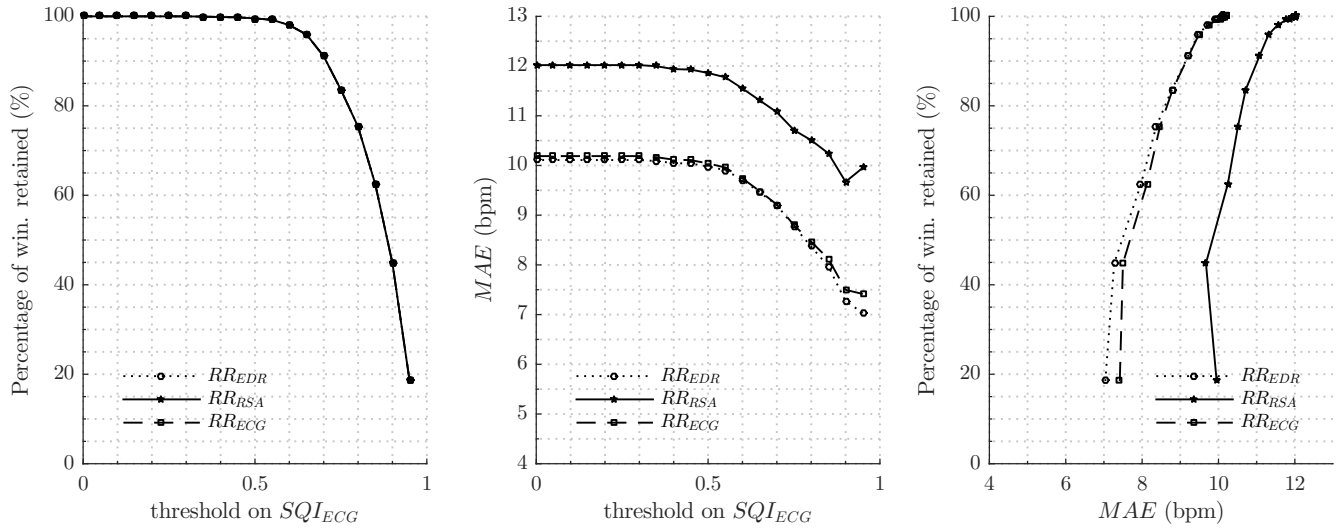


Fig. 5: Relationship between the threshold on SQI_{ECG} , the percentage of windows retained and the mean absolute error (MAE) of retained RR_{EDR} , RR_{RSA} and RR_{ECG} estimates against RR_{ζ} for $RR_{\zeta} \leq 80$ bpm during manual breath counts.

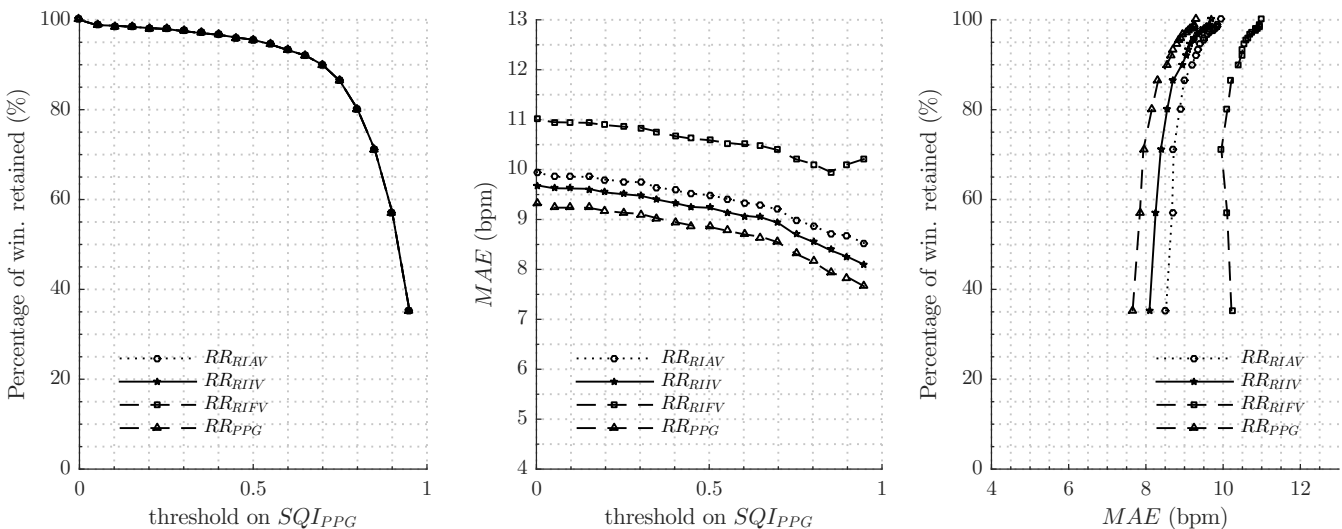


Fig. 6: Relationship between the threshold on SQI_{PPG} , the percentage of windows retained and the mean absolute error (MAE) of retained RR_{RIIV} , RR_{RIAV} , RR_{RIFV} and RR_{PPG} estimates against RR_{ζ} for $RR_{\zeta} \leq 80$ bpm during manual breath counts.

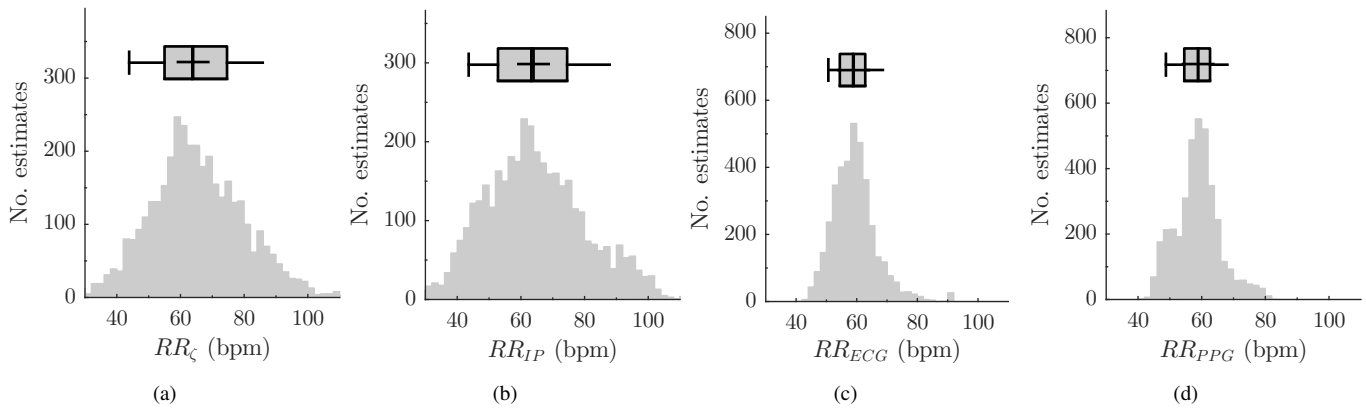


Fig. 7: Distribution of respiratory rate estimates from periods of manual breath counts. Histograms are shown for (a) manual, (b) IP-, (c) ECG-, and (d) PPG-derived rates.

B. Respiratory rate from indirect methods

Figs. 5 and 6 illustrate the reduction in the MAE error for the indirect methods of RR estimation based on the ECG and the PPG when only estimates from windows with progressively higher thresholds in SQI_{ECG} or SQI_{PPG} are considered. For reasons explained later in the paper, this analysis is limited to estimates with $RR_{\zeta} \leq 80$ bpm.

We observed, as expected, that indirect methods based on either source provide RR estimates that are less accurate than those provoked by direct methods based on the IP. Regarding ECG-derived rates, RSA-derived RR has been shown to be less accurate than EDR-derived estimates. This relationship was maintained at all SQI_{ECG} levels. RR_{EDR} and RR_{ECG} (selected from RR_{EDR} and RR_{RSA} using the pole magnitude criterion of [14]), showed similar performance. With respect to the PPG-derived rates, a substantial reduction in MAE was seen across all modulations of this waveform for stricter thresholds on SQI_{PPG} . Of the three sources of modulation of the PPG waveform, the lowest error rates were consistently seen in RIIV estimates (e.g. $MAE(RR_{RIIV}) = 8.3$ bpm at $SQI_{PPG} \geq 0.85$) followed closely by RIAV estimates (e.g. $MAE(RR_{RIAV}) = 8.7$ bpm at $SQI_{PPG} \geq 0.85$). Both were appreciably more accurate than frequency-modulated estimates (e.g. $MAE(RR_{RIFV}) = 9.8$ bpm at $SQI_{PPG} \geq 0.85$). As seen in RR_{ECG} , fusion techniques enabled a reduction in MAE. Using Karlen *et al.*'s criterion, a reduction in MAE of approximately 0.5 bpm in relation to RR extracted from the best-performing source of modulation (RR_{RIIV}) was seen across all SQI thresholds.

C. Distribution of respiratory rates

The distribution of respiratory rates as estimated from all sources for the periods of manual breath counts are shown in Fig. 7. The aliasing effect caused by the undersampling of the respiratory signal at the heartbeat frequency is evidenced by the failure of techniques for RR estimation from PPG or ECG in detecting accurate RR values above 80 bpm.

D. Error analysis

The time series of RR estimates was linearly interpolated at the time instants of RR estimates from the reference measurements (RR_{ζ}) and error metrics were calculated over the time windows of manual counts. Previous papers on respiratory rate estimation from the ECG have reported suboptimal performance at high respiratory rates [14]. Thus, the performance of the RR estimation methods was assessed by calculating error values for two different frequency ranges: (a) $RR_{\zeta} < 80$ bpm (84.7% of windows) and $RR_{\zeta} \geq 80$ bpm (15.4% of windows). The results are summarised in Table II. Only those windows for which the raw signal (IP, ECG or PPG) was reliable were retained for RR estimation. This was achieved by setting the following conditions: $SQI_{ECG} \geq 0.9$, $SQI_{PPG} \geq 0.9$, $SQI_{\psi} \geq 0.9$, $SQI_{IP} \geq 0.9$. As a result, 50.1% of the data was used in validating ECG-derived estimates, 54.7% for PPG-derived estimates, and 54.7% for IP-derived estimates. These thresholds were selected from qualitative analysis of the third column of Figs. 4 through 6 to achieve low MAE rates while retaining a meaningful proportion of estimates (> 50%).

TABLE II: Summary of error analysis for the algorithms for respiratory rate extraction from IP, ECG and PPG-derived respiratory signals. The errors were computed with respect to the reference signal RR_{ζ} . All the figures are shown in breaths-min⁻¹ (bpm).

| Error metrics | Sources | | | |
|---|---------------------|----------------------|----------------------|----------------------|
| | Direct methods | | Indirect methods | |
| | RR_{IP} | RR_{MON} | RR_{ECG} | RR_{PPG} |
| <i>Entire RR_{ζ} range</i> | | | | |
| $ME(\pm SD)$ | -0.8 (± 6.4) | -3.1 (± 12.7) | -7.2 (± 12.5) | -5.5 (± 16.9) |
| MAE | 4.0 | 8.7 | 10.2 | 11.8 |
| <i>$RR_{\zeta} < 80$ bpm</i> | | | | |
| $ME(\pm SD)$ | -0.3 (± 5.6) | -2.2 (± 12.3) | -4.0 (± 11.9) | -0.3 (± 11.9) |
| MAE | 3.6 | 8.2 | 7.5 | 7.8 |
| <i>$RR_{\zeta} \geq 80$ bpm</i> | | | | |
| $ME(\pm SD)$ | -6.0 (± 18.0) | -14.5 (± 19.1) | -31.7 (± 12.6) | -31.2 (± 12.3) |
| MAE | 10.7 | 16.9 | 31.7 | 31.2 |

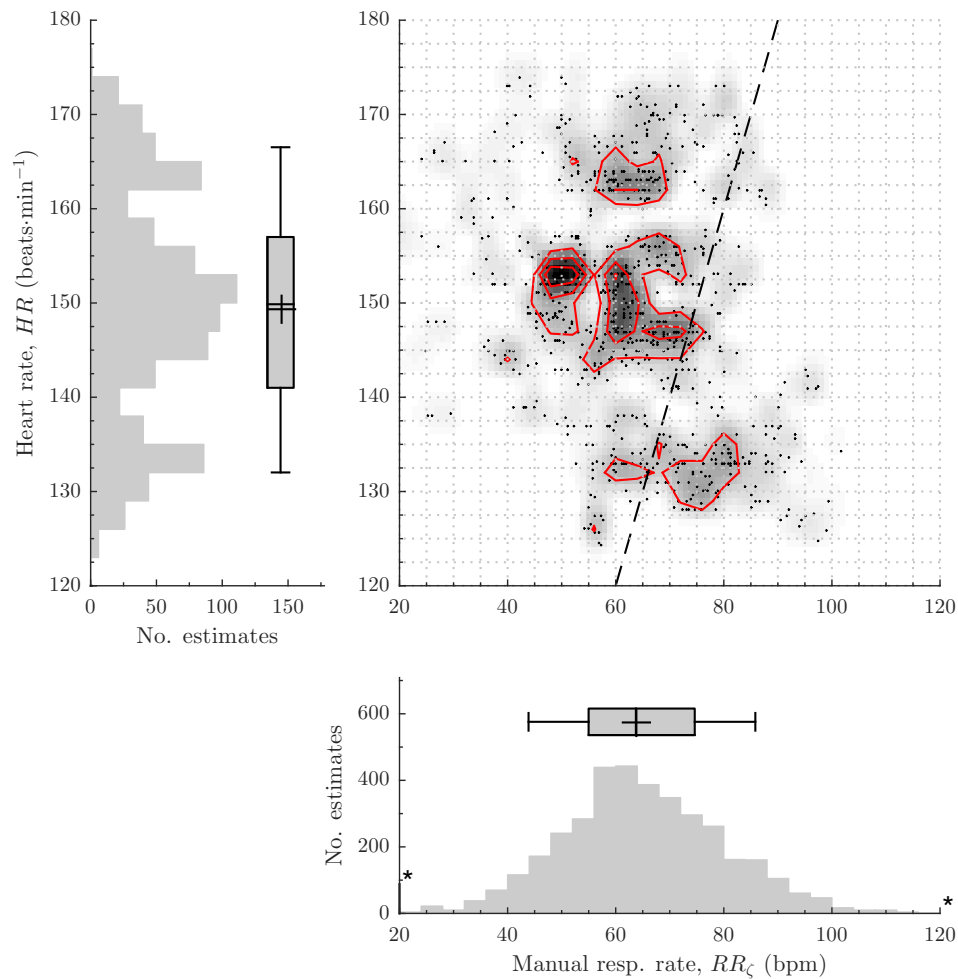


Fig. 8: Heatmap of the distribution of (HR, RR_{ζ}) estimates. Marginal distributions of both variables are also shown. Asterisks represent outliers. The HR values shown were obtained after the cardiac frequency estimates derived by the study monitor for the ECG trace were interpolated at the time instants of RR_{ζ} computation. The red curves represent isolines of the local density of data points. The dark dashed line represents the Nyquist limit for respiratory frequency estimation. For estimates below this line, $RR_{\zeta} > \frac{1}{2}HR$, so the respiratory signal is insufficiently sampled from cardiac beats for accurate detection of the true RR.

V. DISCUSSION

The median reference respiratory rate (computed over manual breath measurements) was found to be 61 bpm (Fig. 7a), with a range extending from 44 to 120 bpm. These figures validate our choice of passband for the digital filters used in RR derivation (20 - 140 bpm). A filter whose passband is slightly wider than the range of frequencies of interest is known to help avoid edge effects near the cut-off frequencies.

When we compare the distribution of RR_{ζ} values in Fig. 7a against the distribution of rates reported by the patient monitor for the entirety of the study period (shown in Fig. 1b), we observe that (a) the median rate obtained during the manual measurements is higher than the median RR_{MON} reported by the patient monitor at the cotside by approximately 8 bpm, and (b) the breathing rates in the 20 - 40 bpm range have not been sampled during the manual breath counts. This was anticipated as this range comprises abnormally low rates that should prompt clinical inspection, and therefore, were not recorded under the stable conditions under which manual counts were scheduled.

We notice also that the range of resting respiratory rates detected is much wider than that found in adults at rest (12 - 20 bpm [49]). The immaturity of the respiratory centres in the lower brainstem of the

premature infant leads to frequent periods of fast shallow breathing, and hence to fast-changing respiratory rates. This renders the problem of accurate RR estimation in this population much more challenging than in the adult population.

A. Errors associated with direct methods

We have re-derived RR from the raw IP signal using standard algorithms for RR extraction found in the literature. It was surprising to note the lower error rates of the RR estimates derived in this manner in relation to those provided by the patient monitor during manual breath counts (Fig. 4); with $MAE(RR_{IP}) = 3.6$ bpm versus $MAE(RR_{MON}) = 8.2$ bpm for $RR_{\zeta} < 80$ bpm and $MAE(RR_{IP}) = 10.7$ bpm versus $MAE(RR_{MON}) = 16.9$ bpm for $RR_{\zeta} \geq 80$ bpm (Table II).

This result suggests that there is room for improvement in the manufacturer's built-in software for deriving respiratory rates in premature infants. The discrepancy between the error rates in RR_{IP} and RR_{MON} was observed even when no IP signal windows were discarded based on poor signal quality. For this reason, the better performance of RR_{IP} over RR_{MON} cannot be attributed to our use of a signal quality index to differentiate between artefactual and non-artefactual windows.

B. Errors associated with indirect methods

Two data fusion methods were adopted to estimate RR from the rates derived from amplitude and frequency modulations of the ECG and PPG waveforms. In both cases, the mean absolute error was reduced as a result of the use of the data fusion approach (Figs. 5 and 6), although this reduction is greater in the case of fused PPG-derived estimates. Nevertheless, the accuracy achieved by both methods was lower than that seen in IP-based estimates of RR (Table II). The differences in the error rates reported were less pronounced in the low RR range ($RR_{\zeta} < 80$ bpm) than in the higher range ($RR_{\zeta} \geq 80$ bpm), as shown in the bottom two rows of Table II.

C. Errors associated with different RR ranges

We calculated the RR estimation errors for two frequency ranges of respiratory rates. The lowest error rates were found for $RR_{\zeta} < 80$ bpm. It is clear from the analysis of Table II that none of the algorithms evaluated based on indirect methods, *i.e.* for either ECG or PPG, could detect rates above this value (note that for $RR_{\zeta} \geq 80$ bpm, ME \simeq MAE values are seen for both ECG and PPG-derived methods).

Both indirect methods suffer from one drawback. As the respiratory signal is only sampled once per cardiac beat, in order for these methods to reveal the fundamental frequency of this signal, this frequency cannot exceed half of the instantaneous heart rate – measured in beats per minute ($\text{beats} \cdot \text{min}^{-1}$) – during the same time epoch. However, a retrospective analysis of the joint distribution of (HR, RR) values during the periods of manual breath counts revealed that instances in which this condition was not observed were not uncommon for this patient group (Fig. 8).

As shown in Fig. 1a, the HR measured in the study cohort has a bell-shaped distribution with a sample median of approximately $157 \text{ beats} \cdot \text{min}^{-1}$. Thus, in instances where the respiratory frequency exceeds half this frequency (approximately 80 bpm), the extraction of RR through indirect methods is likely to be affected by temporal aliasing. In fact, some degree of aliasing of RR estimates by PPG and ECG-based techniques at frequencies as low as 65 bpm as a result of this phenomenon is also to be expected from the analysis of Fig. 8. This suppression of indirect RR estimates is also clear when Fig. 7a and 7b are compared to Fig. 7c and 7d.

D. Errors associated with amplitude-based respiration sources

We found that MAE errors were lower for RR_{IP} when compared to amplitude-based signals, *i.e.* RR_{RIAV} , RR_{RIIV} , and RR_{EDR} (Fig. 4 to 6). In contrast to the protocol of volunteer studies, where subjects are compliant, subject motion during this observational study was largely unrestricted. Motion unrelated to respiration but within the range of breathing frequencies causes amplitude variations that contaminate the amplitude modulation of the detected signals, which ultimately has a deleterious effect on the accuracy of amplitude-based estimates of RR. This may help explain the poor performance of this class of methods in this study.

Given the arrangement of IP/ECG electrodes, an association in the presence of motion noise between these sources was expected. This was confirmed by the comparable percentages of ECG and IP windows retained (50.1 % and 54.7 %, respectively) after thresholds were set on the applicable SQIs. Furthermore, the similar percentage of PPG windows retained (54.7 %) suggests the same artefacts may also affect the PPG sensor, for example, as a result of compound body movement. Further research would be needed to investigate whether a temporal relationship exists between the signal quality of these sources.

E. Errors associated with frequency-based respiration sources

The highest errors were found for methods based on frequency-based sources (RR_{RIFV} and RR_{RSA}), which rely on the RSA as a pathway to respiration. There are conflicting reports in the literature regarding the presence of RSA in preterm infants. Several studies which have estimated RSA in neonates [50] suggest that although there is an interaction between heart rate variability and respiration, this cardiorespiratory interaction is not as continuous as in adults, and may only develop later in some infants. In fact, it has been suggested that RSA may serve to gauge the developmental maturity in neonatal intensive care patients [51]. The evidence for the use of RSA in the continuous monitoring of RR in neonates is scarce [16, 52]. Monasterio *et al.* [37] included both pulse rate and heart rate variability as features in a classifier for apnoea-related desaturations in preterm infants, nevertheless the reliability of these two signals was not assessed against a respiration standard.

VI. CONCLUSIONS

The immaturity of the brain mechanisms governing the respiratory rhythm in preterm infants results in irregular breathing patterns. In neonatal clinical practice, monitoring the breathing pattern of preterm infants allows for a better recognition of physiological instability, and so can provide valuable insights into the cardiorespiratory status of the neonate as well as their maturation level.

The respiratory assessment of the neonate involves primarily the measurement of respiratory rate. In this paper, we have estimated respiratory rates from the three different signal sources available to the patient monitors commonly used in neonatal practice (ECG, PPG, and IP). We excluded periods of poor signal quality, as identified by motion-sensitive signal quality indices. At all times when the infant was at rest (73.1% of time windows), we assessed the performance of previously developed techniques for RR derivation from all signal sources against the reference manual respiratory rates RR_{ζ} during 165 manual breath counts. To our knowledge, this is the first study to assess the performance of these methods against the reference standard of manual respiratory assessments. The work reported has demonstrated a stark performance difference between direct and indirect methods (*i.e.* based on the analysis of the ECG or the PPG signal) at different frequency ranges of respiratory rate. While comparable error rates were found between RR estimates derived using indirect methods and those derived from analysis of the IP signal in the 40 - 80 bpm frequency range (with mean absolute error rates of 7.5 bpm for ECG-derived estimates, 7.8 bpm for PPG-derived estimates, and 3.6 bpm for IP-derived estimates at this range), we nevertheless observed that the measurement of respiratory rate in this population using indirect methods poses a fundamental challenge at fast breathing regimes (upwards of 80 bpm) due to aliasing effects.

These findings have critical implications for the development of indirect methods for RR monitoring in neonatal units as they evidence the performance limits of RR estimates delivered by the ECG and PPG sources currently available in these units. While further studies are required to assess how well our results would generalise to the entire neonatal population, we believe our results should motivate such studies as well as inform the design of alternative non-invasive solutions for the physiological monitoring of these patients.

ACKNOWLEDGMENT

The authors would like to acknowledge the assistance of the Research Nurses in the Neonatal Unit at the John Radcliffe Hospital, Oxford (Sara Davis, Sheula Barlow, and Sharon Garrett) and the families of the participants in the MONITOR Study - Research Ethics Committee: 13/SC/0597.

APPENDIX I PARSING THE KEY LOGS

This appendix describes the processes used to parse the keylogger files produced in order to (a) identify counting cycles, (b) eliminate key presses associated with UI operation, and (c) remove aborted counting cycles.

To achieve (a), key logs were split into individual counting cycles by defining a maximum interval between keystrokes belonging to the same cycle (8 s). As a result of this parsing, 209 manual counting cycles were identified in the 14 recording sessions on 5 study subjects for which the manual respiratory measurements had been logged (Fig. 9a). Manual measurements were taken during periods for which the infants were stable and at rest (*i.e.* the signal of interest is the *resting* respiratory rate). This may explain the discrepancy in the total number of measurements performed from session to session evidenced in Fig. 9a.

In our analysis, we were careful to only include counting cycles carried to completion. Although our protocol specified 40-breath counts, a considerable number of counting cycles was found with

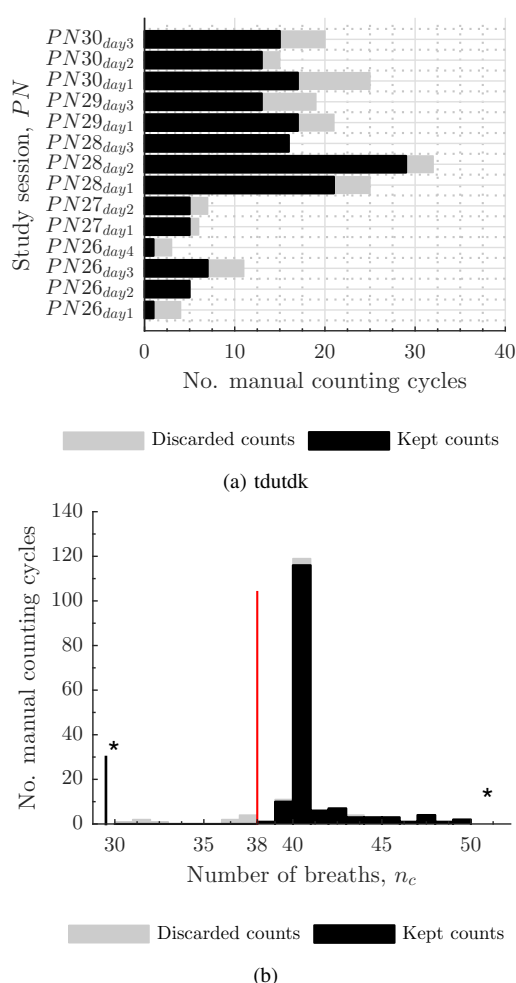


Fig. 9: Effects of application of the selection criteria defined on (9a) the distribution of the total number of manual counting cycles over the study sessions of NICU subjects PN 26 - 30, and (9b) the distribution of the total number of breaths over manual counting cycles. While most counts include upwards of 40 breaths, some shorter counts were concluded before this number was reached. Discarded counts with over 38 breaths were due to the absence of physiological records in the course of the respiratory assessment.

TABLE III: Confusion matrix of complete manual counting cycles (with upwards of 38 breaths) *versus* recording status.

| Manual counts | Recording off | Recording on | Total |
|---------------|---------------|--------------|-------|
| < 38 breaths | 0 | 39 | 39 |
| ≥ 38 breaths | 5 | 165 | 170 |
| Total | 5 | 204 | 209 |

a total of $n_c = 38$ or $n_c = 39$ breaths (Fig. 9b). We hypothesize that a mismatch of a mere couple of breaths is likely to be due to human error, rather than the count being aborted for one of the reasons specified in the study protocol. Thus, cycles composed of fewer than 38 keystrokes (see Fig. 9b) were considered to have been either a result of casual UI operation (case (b)) or aborted by the attending clinical staff due to excessive wriggling, infant motion or other factors which rendered breathing motion imperceptible (case (c)).

Manual counts performed when the recording apparatus was not in use were also discarded. Table III presents a breakdown of counts under each of these categories. After both selection criteria were applied, a total of 165 manual counts were considered for further analysis.

REFERENCES

- [1] A. K. Pramanik, N. Rangaswamy, and T. Gates, "Neonatal respiratory distress: a practical approach to its diagnosis and management." *Pediatric clinics of North America*, vol. 62, no. 2, pp. 453–69, 2015.
- [2] F. F. Rubaltelli, C. Dani, M. F. Reali, G. Bertini, L. Wiechmann, M. Tangucci, and A. Spagnolo, "Acute neonatal respiratory distress in Italy: a one-year prospective study. Italian Group of Neonatal Pneumology." *Acta Paediatrica*, vol. 87, no. 12, pp. 1261–1268, 1998.
- [3] A. Kumar and B. V. Bhat, "Epidemiology of respiratory distress of newborns." *Indian Journal of Pediatrics*, vol. 63, no. 1, pp. 93–98, 1996.
- [4] A. Parkash, N. Haider, Z. A. Khoso, and A. S. Shaikh, "Frequency, causes and outcome of neonates with respiratory distress admitted to neonatal intensive care unit, national institute of child health, Karachi," *Journal of the Pakistan Medical Association*, vol. 65, no. 7, pp. 771–775, 2015.
- [5] L. L. Qian, C. Q. Liu, Y. X. Guo, Y. J. Jiang, L. M. Ni, S. W. Xia, X. H. Liu, W. Z. Zhuang, Z. H. Xiao, S. N. Wang, X. Y. Zhou, and B. Sun, "Current status of neonatal acute respiratory disorders: A one-year prospective survey from a Chinese neonatal network," *Chinese Medical Journal*, vol. 123, no. 20, pp. 2769–2775, 2010.
- [6] J. Ersch, M. Roth-Kleiner, P. Baekert, and H. U. Bucher, "Increasing incidence of respiratory distress in neonates," *Acta Paediatrica, International Journal of Paediatrics*, vol. 96, no. 11, pp. 1577–1581, 2007.
- [7] T. H. Warburton D, Stark AR, "Apnea monitor failure in infants with upper airway obstruction," *Pediatrics*, vol. 60, no. 5, pp. 742–4, 1977.
- [8] R. T. Brouillette, A. S. Morrow, D. E. Weese-Mayer, and C. E. Hunt, "Comparison of respiratory inductive plethysmography and thoracic impedance for apnea monitoring," *The Journal of Pediatrics*, vol. 111, no. 3, pp. 377–383, 1987.
- [9] J. a. Hirsch and B. Bishop, "Respiratory sinus arrhythmia in humans: how breathing pattern modulates heart rate," *Physiology*, vol. 241, no. 4, pp. H620–H629, 1981.
- [10] G. B. Moody and R. G. Mark, "Derivation of respiratory signals from multi-lead ECGs," *Computers in Cardiology*, vol. 12, pp. 113–116, 1985.
- [11] D. J. Meredith, D. Clifton, P. Charlton, J. Brooks, C. W. Pugh, and L. Tarassenko, "Photoplethysmographic derivation of respiratory rate: a review of relevant physiology," *Journal of Medical Engineering & Technology*, vol. 36, no. 1, pp. 1–7, 2012.
- [12] L. G. Lindberg, H. Ugnell, and P. A. Oberg, "Monitoring of respiratory and heart rates using a fibre-optic sensor," *Medical and Biological Engineering and Computing*, vol. 30, no. 5, pp. 533–537, 1992.
- [13] W. Karlen, S. Raman, J. M. Ansermino, and G. a. Dumont, "Multiparameter respiratory rate estimation from the photoplethysmogram," *IEEE Transactions on Biomedical Engineering*, vol. 60, no. 7, pp. 1946–53, 2013.
- [14] C. Orphanidou, S. Fleming, S. Shah, and L. Tarassenko, "Data fusion for estimating respiratory rate from a single-lead ECG," *Biomedical Signal Processing and Control*, vol. 8, no. 1, pp. 98–105, 2013.

- [15] E. Olsson, H. Ugnell, P. a. Oberg, and G. Sedin, "Photoplethysmography for simultaneous recording of heart and respiratory rates in newborn infants," *Acta Paediatrica*, vol. 89, no. 7, pp. 853–861, 2000.
- [16] A. Johansson, P. A. Oberg, and G. Sedin, "Monitoring of heart and respiratory rates in newborn infants using a new photoplethysmographic technique," *Journal of Clinical Monitoring and Computing*, vol. 15, no. 7-8, pp. 461–467, 1999.
- [17] J. Lázaro and E. Gil, "Deriving respiration from the pulse photoplethysmographic signal," *Computing in Cardiology*, vol. 38, pp. 713–716, 2011.
- [18] S. Fleming, L. Tarassenko, M. Thompson, and D. Mant, "Non-invasive measurement of respiratory rate in children using the photoplethysmogram," *Proceedings of the Annual International Conference of IEEE Engineering in Medicine and Biology Society*, vol. 2008, pp. 1886–1889, 2008.
- [19] S. G. Fleming and L. Tarassenko, "A comparison of signal processing techniques for the extraction of breathing rate from the photoplethysmogram," *International Journal of Biological and Life Sciences*, vol. 2, no. 4, pp. 233–237, 2006.
- [20] A. Schäfer and K. W. Kratky, "Estimation of breathing rate from respiratory sinus arrhythmia: Comparison of various methods," *Annals of Biomedical Engineering*, vol. 36, no. 3, pp. 476–485, 2008.
- [21] J. Thayer, I. Sollers, J.J., E. Ruiz-Padial, and J. Vila, "Estimating respiratory frequency from autoregressive spectral analysis of heart period," *IEEE Engineering in Medicine and Biology Magazine*, vol. 21, no. 4, pp. 41–45, 2002.
- [22] C. L. Mason and L. Tarassenko, "Quantitative assessment of respiratory derivation algorithms," *Proceedings of the 23rd Annual International Conference of the IEEE Engineering in Medicine and Biology Society*, pp. 1998–2001, 2001.
- [23] S. B. Park, Y. S. Noh, S. J. Park, and H. R. Yoon, "An improved algorithm for respiration signal extraction from electrocardiogram measured by conductive textile electrodes using instantaneous frequency estimation," *Medical and Biological Engineering and Computing*, vol. 46, no. 2, pp. 147–158, 2008.
- [24] A. Garde, W. Karlen, J. M. Ansermino, and G. A. Dumont, "Estimating respiratory and heart rates from the correlogram spectral density of the photoplethysmogram," *PLoS ONE*, vol. 9, no. 1, pp. 1–11, 2014.
- [25] S. Nemati, A. Malhotra, and G. D. Clifford, "Data fusion for improved respiration rate estimation," *European Association for Signal Processing Journal on Advances in Signal Processing*, vol. 2010, p. 926305, 2010.
- [26] S. A. Shah, S. Fleming, M. Thompson, and L. Tarassenko, "Respiratory rate estimation during triage of children in hospitals," *Journal of Medical Engineering and Technology*, vol. 39, pp. 514–524, 2015.
- [27] P. A. Leonard, J. G. Douglas, N. R. Grubb, D. Clifton, P. S. Addison, and J. N. Watson, "A fully automated algorithm for the determination of respiratory rate from the photoplethysmogram," *Journal of Clinical Monitoring and Computing*, vol. 20, no. 1, pp. 33–36, 2006.
- [28] J. Pan and W. Tompkins, "A real-time QRS detection algorithm," *Biomedical Engineering, IEEE*, vol. 32, no. 3, pp. 230–236, 1985.
- [29] W. Zong, "A robust open-source algorithm to detect onset and duration of QRS Complexes," *Computers in Cardiology*, 2003.
- [30] G. Moody, "The MIT.BIH Arrhythmia database on CD-ROM and software for use with IT," 1990.
- [31] W. Zong, T. Heldt, G. Moody, and R. Mark, "An open-source algorithm to detect onset of arterial blood pressure pulses," *Computers in Cardiology*, pp. 259–262, 2003.
- [32] M. Aboy, J. McNames, T. Thong, D. Tsunami, M. S. Ellenby, and B. Goldstein, "An automatic beat detection algorithm for pressure signals," *IEEE Transactions on Biomedical Engineering*, vol. 52, no. 10, pp. 1662–1670, 2005.
- [33] B. N. Li, M. C. Dong, and M. I. Vai, "On an automatic delineator for arterial blood pressure waveforms," *Biomedical Signal Processing and Control*, vol. 5, no. 1, pp. 76–81, 2010.
- [34] W. Karlen, J. M. Ansermino, and G. D. Fellow, "Adaptive pulse segmentation and artifact detection in photoplethysmography for mobile applications," in *Proceeding of the 34th Annual International Conference of the IEEE Engineering in Medicine and Biology*. IEEE EMBS, 2012, pp. 3131–3134.
- [35] I. I. Goncharova and J. S. Barlow, "Changes in EEG mean frequency and spectral purity during spontaneous alpha blocking," *Electroencephalography and Clinical Neurophysiology*, vol. 76, no. 3, pp. 197–204, 1990.
- [36] E. Gil, J. María Vergara, and P. Laguna, "Detection of decreases in the amplitude fluctuation of pulse photoplethysmography signal as indication of obstructive sleep apnea syndrome in children," *Biomedical Signal Processing and Control*, vol. 3, no. 3, pp. 267–277, 2008.
- [37] V. Monasterio, F. Burgess, and G. D. Clifford, "Robust classification of neonatal apnoea-related desaturations," *Physiological Measurement*, vol. 33, no. 9, pp. 1503–1516, 2012.
- [38] B. Hjorth, "EEG analysis based on time domain properties," *Electroencephalography and Clinical Neurophysiology*, vol. 29, no. 3, pp. 306–310, 1970.
- [39] L. Sornmo and P. Laguna, *Bioelectrical signal processing in cardiac and neurological applications*. Academic Press, 2014, vol. 16.
- [40] A. V. Deshmane, "False arrhythmia alarm suppression using ECG, ABP, and photoplethysmogram," Master's thesis, Massachusetts Institute of Technology, 2009.
- [41] Q. Li, R. G. Mark, and G. D. Clifford, "Robust heart rate estimation from multiple asynchronous noisy sources using signal quality indices and a Kalman filter," *Physiological Measurement*, vol. 29, no. 1, pp. 15–32, 2008.
- [42] J. Behar, J. Oster, Q. Li, and G. D. Clifford, "ECG signal quality during arrhythmia and its application to false alarm reduction," *IEEE Transactions on Biomedical Engineering*, vol. 60, no. 6, pp. 1660–1666, 2013.
- [43] Q. Li and G. D. Clifford, "Dynamic time warping and machine learning for signal quality assessment of pulsatile signals," *Physiological Measurement*, vol. 33, no. 9, pp. 1491–1501, 2012.
- [44] L. Zhao, S. Reisman, and T. Findley, "Derivation of respiration from electrocardiogram during heart rate variability studies," in *Computers in Cardiology*, 1994, pp. 53–56.
- [45] A. Travaglini, C. Lamberti, J. DeBei, and M. Ferri, "Respiratory signal derived from eight-lead ECG," *Computers in Cardiology*, p. 4, 1998.
- [46] D. Cysarz, R. Zerm, H. Bettermann, M. Frühwirth, M. Moser, and M. Kröz, "Comparison of respiratory rates derived from heart rate variability, ECG amplitude, and nasal/oral airflow," *Annals of Biomedical Engineering*, vol. 36, no. 12, pp. 2085–2094, 2008.
- [47] S. M. Kay and S. L. J. Marple, "Spectrum analysis—A modern perspective," *Proceedings of the IEEE*, vol. 69, no. 11, pp. 1380–1419, 1981.
- [48] J. P. Burg, "Maximum entropy spectral analysis," *Proceedings of the 37th Annual International SEG Meeting*, vol. 6, p. 0, 1975.
- [49] A. C. Guyton, J. E. Hall, and J. P. Fisher, *Respiration: ventilation, circulation, & transport*, 11th ed., John P. Fisher, Ed. Saunders, 2012.
- [50] P. Indic, D. Paydarfar, and R. Barbieri, "Point process modeling of interbreath interval: A new approach for the assessment of instability of breathing in neonates," *IEEE Transactions on Biomedical Engineering*, vol. 60, no. 10, pp. 2858–2866, 2013.
- [51] M. T. Clark, C. G. Rusin, J. L. Hudson, H. Lee, J. B. Delos, L. E. Guin, B. D. Vergales, a. Paget-Brown, J. Kattwinkel, D. E. Lake, and J. R. Moorman, "Breath-by-breath analysis of cardiorespiratory interaction for quantifying developmental maturity in premature infants," *Journal of Applied Physiology*, vol. 112, no. 5, pp. 859–867, 2012.
- [52] D. Wertheim, C. Olden, E. Savage, and P. Seddon, "Extracting respiratory data from pulse oximeter plethysmogram traces in newborn infants," *Archives of Disease in Childhood - Fetal and Neonatal edition*, vol. 94, no. 4, pp. F301–F303, 2009.